4th International Conference on Structural Health Monitoring of Intelligent Infrastructure (SHMII-4) 2009
22-24 July 2009, Zurich, Switzerland

Dynamic identification and damage detection of a RC building subjected to earthquake excitation

F. Cavalieri[1], M. Imbimbo[1], R. Betti[2], and C. C. Lin[3]

1 Department of Mechanics, Structures and Environment, University of Cassino, Cassino (FR), Italy
2 Department of Civil Engineering and Engineering Mechanics, Columbia University, New York, NY, 10027, USA
3 Department of Civil Engineering, National Chung Hsing University, Taichung, Taiwan 40227

ABSTRACT: In this paper are presented the results of an experimental study concerning the dynamic identification and the damage assessment of a real building. The considered structure is the building of the Civil and Environmental Engineering Department at NCHU in Taichung which was subjected, between July 1998 and November 1999, to the Chi-Chi Earthquake main shock and numerous foreshocks and aftershocks. The building is instrumented by a monitoring system composed of 29 accelerometers. The dynamic identification is, first, performed through the FDD (Frequency Domain Decomposition) method by using only the output records according to the Operational Modal Analysis. Then, the OKID-ERA/DC time domain algorithm is applied as well, using the output accelerations together with the other available records considered as input base accelerations. Based on the identification results, some linear and nonlinear damage indexes are applied providing an indication about the presence and location of damage. The main goal of the investigation is to test the efficacy of the analysed identification techniques and damage indexes in a real case.

1 INTRODUCTION

Most existing structures show damage following the occurrence of an earthquake. If damage is not detected and rectified a critical condition can occur, eventually resulting in catastrophic structural failure. In this context, structural system identification plays an important role. At present many identification and damage detection methodologies are available from the literature. However, there are not many applications to real cases, since not all the buildings are instrumented for strong motion monitoring and not all the monitored ones are subjected to an earthquake excitation.

In this work some of the identification and damage detection methodologies are tested with reference to a real case study. In particular, two types of approach, linear and nonlinear, are discussed. According to the linear one, the FDD method and the OKID-ERA/DC algorithm are presented and applied to the structure both in the undamaged and damaged states. Then, on the basis of the retrieved dynamic parameters, some of the most efficient linear damage indexes are discussed. Following the nonlinear approach, a data-driven technique, which does not require any hypothesis on the structural model and can account of structural nonlinearity, is presented and applied. The approach is based only on one record of the output signals and provides an assessment of the damage along all of the monitored dofs on the basis of the residuals between the recorded signals and the predicted ones, both in time and in frequency domain.

2 CASE STUDY: THE CEED BUILDING AT NCHU

The structure analysed in this work is the building of the Civil and Environmental Engineering Department (CEED) at the National Chung Hsing University (NCHU) in Taichung, Taiwan. It is a seven-story reinforced concrete building, with a basement and a roof floor. To this building, a smaller three-story building is connected along the short side. The base dimensions of the main building are 57 m × 37.5 m, with a height of 26.8 m above ground. This structure was subjected, between July 1998 and November 1999, to the Taiwan Chi-Chi Earthquake main shock and numerous foreshocks and aftershocks, and experienced moderate structural damage, including the damage of partition walls and the separation of walls from columns and floor beams in the lower stories.

This building was instrumented in 1990 for strong motion monitoring with 29 accelerometers the locations of which are shown in Figure 1: eight sensors on the basement, six sensors on the ground level, six on the 4th floor, six on the roof, and three sensors on the free field (E-W, N-S and Up-Down directions), at a location far from the building, which can be considered representative of the free-field ground motion. In this study, since the interest is focused on the main seven-story building, the structural responses recorded at the eight sensors located in the x and y directions on the 4th floor (Channels 12, 13, 14 and 15) and roof (Channels 18, 19, 21, 22), are used as output sets. For simplicity, in the next sections of the paper, the registered channels are named as the dofs reported in Table 1.

Table 1. Scheme of employed channels and correspondent dofs

Floor	Direction	Registered Channel	Dof	Registered Channel	Dof
4th floor	x	13	2	15	4
4th floor	y	12	1	14	3
Roof	x	19	6	22	8
Roof	y	18	5	21	7

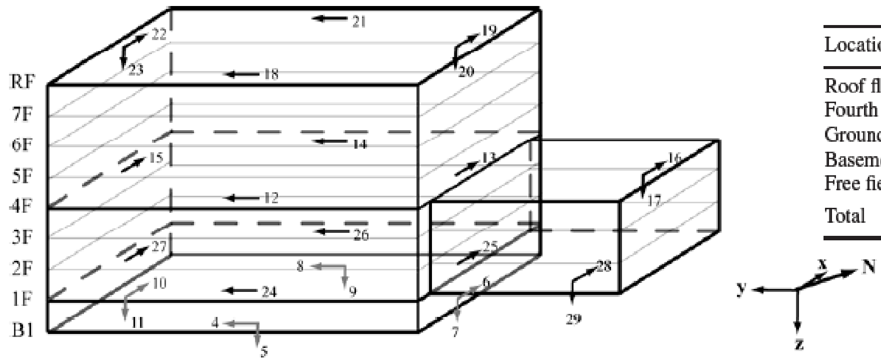

Location	Number of channels
Roof floor	6 (2EW, 2NS, 2V)
Fourth floor	6 (2EW, 3NS, 1V)
Ground level	6 (2EW, 3NS, 1V)
Basement	8 (2EW, 2NS, 4V)
Free field	3 (1EW, 1NS, 1V)
Total	29

Figure 1. Sensor locations in the NCHU CEED building.

The time histories recorded at the four sensors located in the x and y directions on the first floor (Ch 24, 25, 26, 27), if considered as outputs, do not provide any additional valuable information in terms of global behavior of the building and, hence, were not included in the output sets. The input sensor set is chosen to be composed of the eight sensors at the basement. This choice, already adopted in Hong et al. (2008) as “Flexible Base” Analysis (FBA), allows to account for the flexibility of the foundation mat and include the soil-structure interaction effects on the dynamic behavior of the building. Among the available data sets, in this work the 07/07/1999 and 10/19/1999 recorded signals (small energy foreshock and aftershock, respectively) have been used for the application of the linear approach, while in the nonlinear approach the 09/21/1999 main shock data set was used.

3 LINEAR APPROACH

In the following, it is presented the linear approach used in this work to assess the potential structural damage. Two of the most common identification techniques for linear systems, are briefly introduced and applied to the CEED building. Based on the identification results, some linear indexes are applied. These indexes require the use of two records, in the undamaged and damaged states, and do not account of structural nonlinearity. In the following, the undamaged or reference case will be named to as RC, while the damaged one as DC.

3.1 Identification techniques

3.1.1 Frequency Domain Decomposition

According to the FDD (Frequency Domain Decomposition) method, for each frequency a SVD (Singular Values Decomposition) of the output PSD (Power Spectral Density) matrix is performed and the first singular values (SV) of each matrix are plotted against frequency. By applying the Peak Picking to this plot it is possible to obtain the mode shapes and the damped natural frequencies of the system, while the modal damping ratios for all modes can be estimated through the Half-Power Bandwidth method.

In this work, although the input records are available, the FDD method is performed by using only the output records in order to test the efficiency of this method in the very common case of a real structure with limited instrumentation and unknown input.

In Figure 2a) is reported the first singular values plot in the FDD method, for the RC case. From the figure it is clear that the Peak Picking is difficult to be applied because of the scarcity of the recorded signals, the presence of high noise level and the use of a not white Gaussian input.

A first way to overcome this problem consists of adding different levels of white Gaussian noise to the data and averaging the correspondent noise polluted singular values. The results are reported in Figure 2b) where it can be noted that in correspondence of the structural peaks, the original and the noise polluted SV are closer than in the vicinity of a noisy peak. For a better understanding, in Figure 3 is reported the deviation between the two sets of noise free and noise polluted SV. From the figure it is interesting to note that the analysis of the deviation makes easier to identify the structural peaks and the corresponding eigenfrequencies.

An additional way to discriminate between modal and noise peaks is based on the modal coherence, that is defined by $d(f_0) = v(f)^T \cdot v(f_0)$, where $v(f_0)$ is the first singular vector at the peak of frequency f_0 and $v(f)$ is the first singular vector at neighboring points, at frequency f. Given a threshold level Ω (i.e. equal to 0.8), if the modal coherence at f_0 is larger than Ω, then at the neighboring point the same mode is dominating. In the case of seismic input with not completely uncorrelated time values, the values of $d(f_0)$ are also high in the presence of a noise peak. Therefore the modal coherence can be applied between the first singular vectors without noise and those at the neighboring points on the noise polluted SV plot. The results, in terms of the modal coherence computed for the structural peaks and some noise peaks for the RC case, are reported in Table 2. The table provides an additional information about the structure modal peaks.

The results of the above analyses, in terms of the undamped mode shapes and eigenfrequencies of the system, in the undamaged and damaged case, are reported in Table 3. The results show a good agreement with those computed in the previous study by Hong et al. (2008). In this case it has not been possible to evaluate the modal damping ratios.

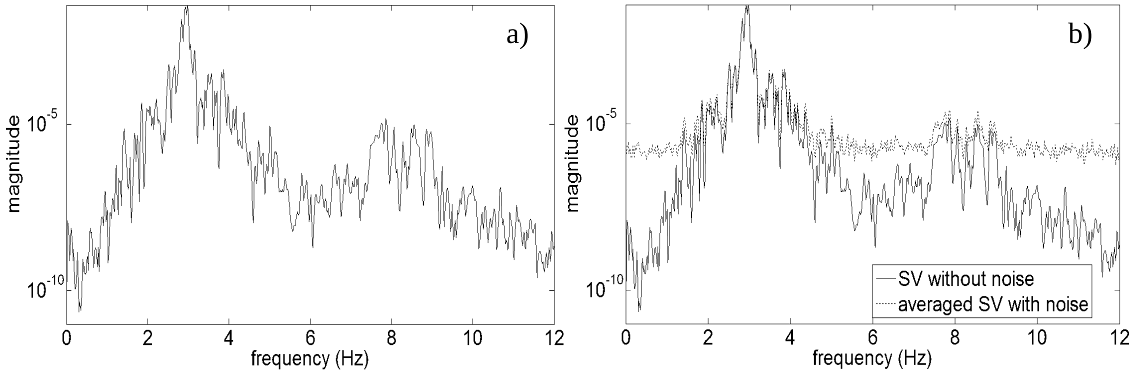

Figure 2: a) – First singular values (RC case); b) – Original and noise polluted singular values (RC case).

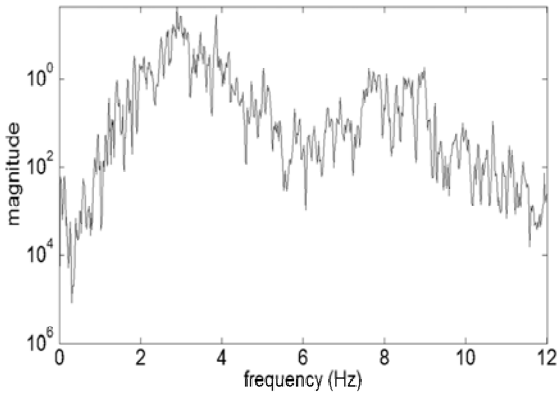

Figure 3: Deviation between original and noise polluted singular values.

Table 2. Modal coherence for some peaks

Frequency Hz	$d(f_0)$	Peak type
2.903	0.930	modal
3.050	0.976	modal
3.474	0.758	noise
3.865	0.957	modal
5.023	0.720	noise
8.986	0.860	modal
9.247	0.962	modal
10.666	0.943	modal

Table 3. Identification results from FDD – RC case on the left, DC case on the right

RC CASE						DC CASE					
FDD undamped mode shapes						FDD undamped mode shapes					
0.292	0.280	0.111	0.127	0.193	0.137	0.333	0.057	0.109	0.441	0.178	0.173
0.094	0.082	-0.238	-0.156	0.189	0.573	0.031	0.122	-0.289	0.043	0.180	-0.379
0.212	-0.199	-0.104	-0.108	0.247	-0.234	0.323	-0.121	-0.110	0.593	-0.201	-0.279
0.254	0.233	0.206	0.483	-0.408	0.268	0.044	0.407	0.181	0.072	0.572	0.547
0.555	0.568	0.301	-0.218	-0.136	-0.195	0.601	0.126	0.237	-0.422	-0.238	-0.203
0.258	0.256	-0.608	0.505	-0.538	-0.449	0.077	0.219	-0.655	-0.053	-0.419	0.382
0.422	-0.437	-0.361	0.135	-0.213	0.289	0.641	-0.308	-0.392	-0.508	0.125	0.284
0.493	0.491	0.536	-0.627	0.589	-0.451	0.071	0.802	0.470	0.089	-0.566	-0.426
FDD eigenfrequencies						FDD eigenfrequencies					
Hz						Hz					
2.903	3.050	3.865	8.986	9.247	10.666	2.173	2.476	3.195	6.630	7.972	9.506

3.1.2 OKID-ERA/DC

In this section, the identification of the system is performed in time domain by using the OKID (Observer Kalman/filter Identification) - ERA/DC (Eigensystem Realization Algorithm with Data Correlation) algorithm. In this case, both input and output data sets are used.

From the Hankel matrix, the system order for both RC and DC cases results equal to 12, corresponding to 6 modes (the first and second bending modes in the x and y directions and the first and second torsional modes). Table 4 shows the identification results in terms of undamped mode shapes, eigenfrequencies and modal damping ratio. The results show a good agreement with those computed in Hong et al. (2008) and are also better than those retrieved from the previous approach based on FDD.

Table 4: Identification results from OKID-ERA/DC – RC case on the left, DC case on the right

RC CASE						DC CASE					
OKID-ERA/DC	undamped mode shapes					OKID-ERA/DC	undamped mode shapes				
0.263	0.212	0.114	0.042	0.453	0.089	0.319	0.080	0.111	0.444	0.061	0.157
0.068	0.086	-0.250	-0.312	0.067	0.463	0.026	0.098	-0.285	0.046	0.233	-0.466
0.237	-0.129	-0.092	-0.107	0.522	-0.168	0.310	-0.072	-0.100	0.573	-0.057	-0.232
0.226	0.324	0.194	0.637	-0.068	0.510	0.022	0.415	0.161	0.040	0.626	0.475
0.534	0.456	0.317	-0.073	-0.426	-0.176	0.609	0.194	0.284	-0.417	-0.124	-0.208
0.174	0.251	-0.661	0.416	-0.145	-0.403	0.062	0.215	-0.711	-0.059	-0.401	0.435
0.523	-0.285	-0.305	0.155	-0.545	0.225	0.651	-0.155	-0.336	-0.541	0.101	0.249
0.479	0.688	0.499	-0.530	0.113	-0.496	0.038	0.836	0.415	0.035	-0.600	-0.429
OKID-ERA/DC	eigenfrequencies					OKID-ERA/DC	eigenfrequencies (Hz)				
Hz						Hz					
3.084	3.112	3.908	8.598	9.295	10.978	2.239	2.548	3.212	6.938	8.076	9.668
OKID-ERA/DC	modal damping ratios					OKID-ERA/DC	modal damping ratios				
0.032	0.021	0.018	0.017	0.016	0.015	0.024	0.022	0.016	0.030	0.033	0.025

3.2 Linear damage indexes

Based on the dynamic parameters retrieved from the OKID-ERA/DC algorithm, some linear damage indexes are applied for the damage assessment of the case study.

3.2.1 Frequency change based indexes

One of the most common method to assess the presence of damage consists of comparing the natural frequencies (ω, ω^d) before and after the event causing the potential damage. In particular, it can be defined the index $freq.\,index_j = \frac{\omega_j^d - \omega_j}{\omega_j}$ for the j-th frequency which provides some information about the presence of damage and the mode more affected by the damage. In Figure 4a) are reported the frequencies for the RC and DC cases for the six modes. The figure shows a reduction of all the frequencies which could suggest that the building experienced damage between the two acquisitions, probably during the Chi-Chi Earthquake main shock and/or one of its aftershocks. In Figure 4b) are reported the values of the *frequency index* for all the six identified modes. The figure shows that all modes change due to damage with a major effect on the first one.

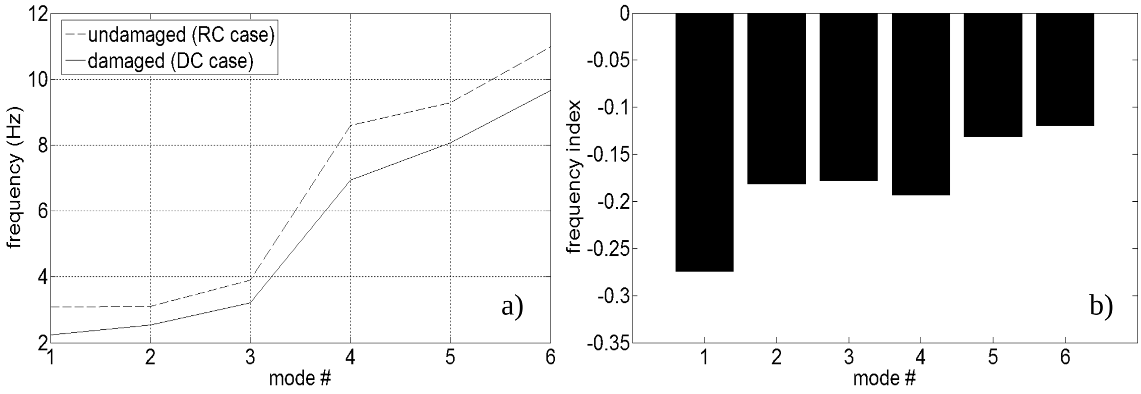

Figure 4: a) – Frequencies for the RC and DC cases; b) – Frequency index for all modes.

3.2.2 Flexibility change based indexes

A localized damage in a structure causes an increase in flexibility. If two measurement sets (for the undamaged and damaged states) are available, it is possible to evaluate the flexibility matrices $\boldsymbol{F}$ and $\boldsymbol{F}^d$ for the two states. Alvin et al. (2003) defined two global indexes, whose highest values give an estimate of the damage position:

$$RDI_1 = \left|diag\left(\boldsymbol{F}^d - \boldsymbol{F}\right)\right| \quad ; \quad RDI_2 = \left|diag\left(\boldsymbol{F}^d - \boldsymbol{F}\right)\right| / \left|diag\left(\boldsymbol{F}\right)\right| \tag{1}$$

Figures 5a) and 5b) show the RDI_1 and RDI_2 plots. All the monitored dofs have non zero values. In particular the highest values are reached along the 1st and 3rd dofs, for the 4th floor, and the 5th and 7th dofs, for the roof. This means that the building has been damaged more in the *y* direction than in the *x* direction although nothing can be said about the position of damage.

From the difference between the flexibility matrices $\boldsymbol{F}$ and $\boldsymbol{F}^d$ of the two states, it can be obtained the change matrix $\boldsymbol{\Delta F}$. For each translational degree of freedom *i*, Pandey et al. (1995) defined the δ_i index, being the maximum absolute value of the elements in the corresponding row of $\boldsymbol{\Delta F}$, i.e. $\delta_i = \max_j \left|\boldsymbol{\Delta F}_{ij}\right|$. The damage is located where it can be seen a large step in the δ_i plot. In Figure 6 it is shown the δ_i plot for the analysed building. The largest steps, indicated by arrows in the figure, concern the 1st and 2nd dofs, the 2nd and 3rd dofs, for the 4th floor, the 5th and 6th dofs, the 6th and 7th dofs, for the roof, confirming a major damage in the *y* direction.

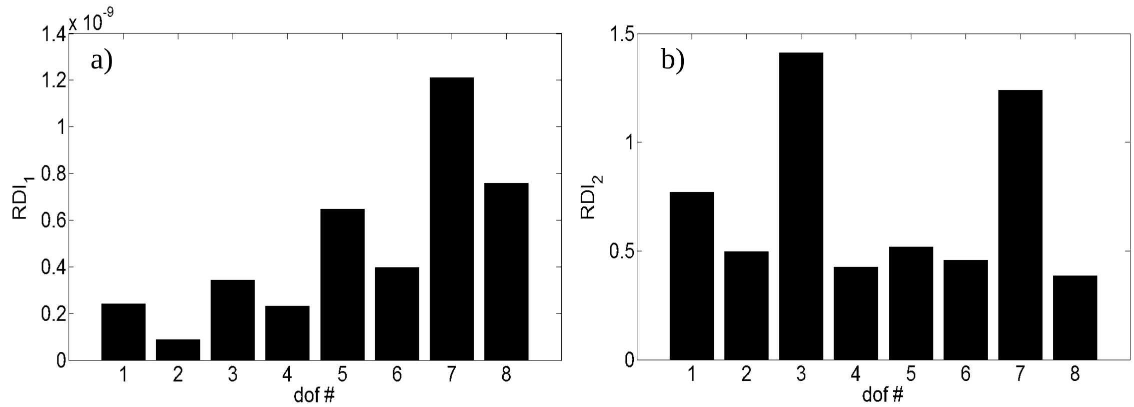

Figure 5: a) – RDI_1 plot; b) – RDI_2 plot.

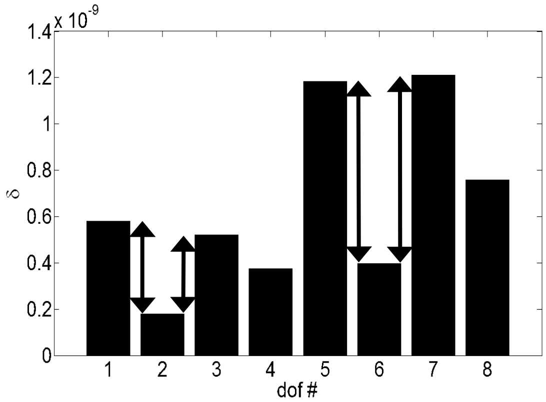

Figure 6: δ_i plot.

4 NONLINEAR APPROACH: DATA DRIVEN TECHNIQUE

When a structure is subjected to an extreme event such as an intense ground shaking it will deform into its inelastic range. Any deviation from linearly-elastic behavior can be considered as a result of the extreme event and hence as “damage”. Therefore, with the aim of checking if the structure is damaged or not, a possible solution could be obtained by comparing the recorded output signals with the predicted ones, under the assumption of linear behavior. Mohamed (2005) proposed that the initial segments of the input and output signals, representing small vibration amplitude, can be used for identifying the linear systems by using the OKID-ERA/DC algorithm. Based on the obtained realization, responses at sensor locations can be predicted for the entire duration of the ground motion. The residuals between each of the recorded signals and the predicted ones under the assumption of linear behavior are given by:

$$\%err_{time} = \left[\sum_{i=1}^{N} \left(y_{recorded} - y_{predicted} \right)^2 \right]^{1/2} \times 100 \qquad (2)$$

Eqn. (2) can be used to extract useful information on the damage state of the structure. The same approach can be used in the frequency domain, computing the residuals between the power spectrum of the recorded signals and the power spectrum of the predicted ones, i.e.:

$$\%err_{frequency} = \left[\sum_{i=1}^{N} \left(power_{y\_recorded} - power_{y\_predicted} \right)^2 \right]^{1/2} \times 100 \qquad (3)$$

Knowing from the literature that the structure was subjected to moderate damage following the Chi-Chi main shock, the 09/21/1999 data set is used to apply the nonlinear damage detection technique to the CEED building. The linear predicted response is first computed, under the main shock input, from the realization obtained by the 07/07/1999 data set. Comparing the recorded outputs with the predicted ones indicates that the predicted response is very close and almost identical to the actual response as long as the structure remains in the linear field. As the response changes from linear to nonlinear, the realization is no more able to predict the structural response. The time domain residuals (2) and the frequency domain residuals (3) are reported in Figures 7a) and 7b) for all the monitored dofs of the analysed building. Both the figures show that the largest deviations are reached along the 1st and 3rd dofs, for the 4th floor, and the 5th and 7th dofs, for the roof. The results from the nonlinear approach, hence, agree with those obtained form the previous linear study and confirm that the building has been damaged more in the *y* direction than in the *x* direction. At the same time the nonlinear approach, as the linear one, does not provide any further information about the location of damage.

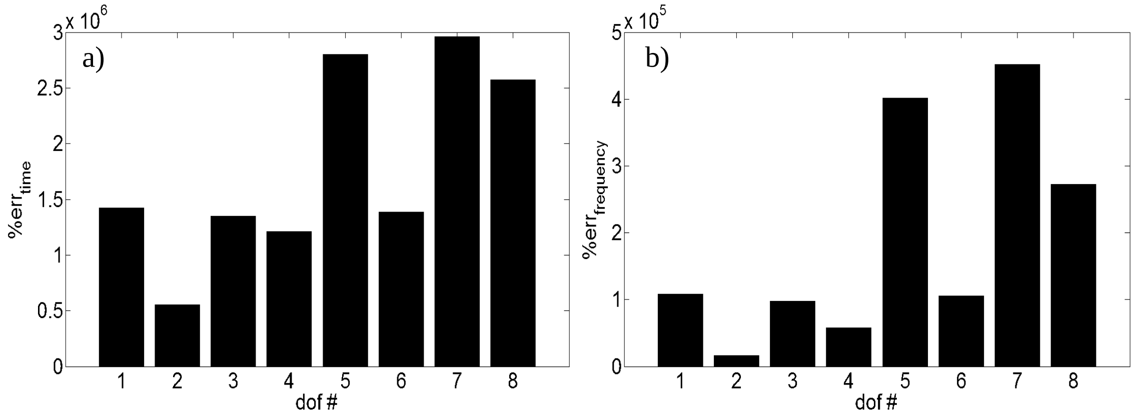

Figure 7: a) – time domain residuals; b) – frequency domain residuals.

5 CONCLUSIONS

In this paper, it is discussed the experimental study conducted on the seven-story reinforced concrete building of the Civil and Environmental Engineering Department at NCHU in Taichung, that between July 1998 and November 1999 was subjected to the Chi-Chi Earthquake main shock and numerous foreshocks and aftershocks. The goal of this investigation was to test the performance of some of the most common identification techniques and damage indexes in a real case study. The system identification has been first performed by the FDD method by using only output records. Then the OKID-ERA/DC has been applied using output and input records. The OKID-ERA/DC proved to be more stable and efficient than the FDD method, also because the analysed structure was subjected to a band limited earthquake base motion, instead of ambient vibration. The system identification techniques applied to the building provided results in good agreement with those available in a previous study on the building. The system identification results has been the base for evaluating some linear and nonlinear damage indexes which gave a clear indication of the most damaged dofs and direction, but, on the basis of the available instrumentation, did not allow to detect the precise position of the damage.

6 REFERENCES

Ueng, JM, Lin, CC, and Lin, PL. 2000. System identification of torsionally coupled buildings. Computers and Structures, 74: 667-686.

Wu, WH, Wang, JF, and Lin, CC. 2001. Systematic assessment of irregular building-soil interaction using efficient modal analysis. Earthquake Engng Struct. Dyn., 30: 573-594.

Lin, CC, Wang, CE, Wu, HW, and Wang, JF. 2005. On-line building damage assessment based on earthquake records. Smart Mater. Struct, 14: S137-S153.

Lin, CC, and Wang, JF. 2008. Dynamic Parameter Identification for Irregular Buildings Considering Soil-Structure Interaction Effects. Earthquake Spectra, 24(3): 641-666.

Hong, AL, Betti, R, and Lin, CC. 2008. Identification of Dynamic Models of a Building Structure using Multiple Earthquake Records. International Symposium on Structural Control and Health Monitoring, Jan 10-11, Taichung, Taiwan.

Mohamed, AS. 2005. *A data driven Approach for Earthquake Damage Detection*. Master's Thesis, The Graduate School of Natural and Applied Sciences, Atilim University.

Pandey, AK, and Biswas, M. 1995. Experimental Verification of Flexibility Difference Method for Locating Damage in Structures. Journal of Sound and Vibration, 184(2): 311-328.

Alvin, KF, Robertson, AN, Reich, GW, and Park, KC. 2003. Structural system identification: from reality to models. Computers and Structures, 81: 1149-1176.